

PUBLISHED VERSION

M.J. Emes, M. Arjomandi, R.M. Kelso and F. Ghanadi

Integral length scales in a low-roughness atmospheric boundary layer

Proceedings of the 18th Australasian Wind Engineering Society Workshop, 2016 / pp.1-4

© The Australasian Wind Engineering Society, all rights reserved.

PERMISSIONS

Permission granted (The author will hold full rights for self-archiving of their paper) via email on 13 November, 2017 from Australasian Wind Engineering Society to **add full text** (pdf) of this paper from the 18th Australasian Wind Engineering Society Workshop (18th : 2016 : McLaren Vale, South Australia).

13 November 2017

<http://hdl.handle.net/2440/109454>

Integral Length Scales in a Low-Roughness Atmospheric Boundary Layer

M.J. Emes, M. Arjomandi, R.M. Kelso and F. Ghanadi

School of Mechanical Engineering
 University of Adelaide, Adelaide, South Australia 5005, Australia

Abstract

This paper discusses the integral length scales in a low-roughness atmospheric boundary layer (ABL), based on the high-fidelity measurements of wind velocity. Results from the analysis shows that longitudinal integral length scales follow a linear relationship with height in a low-roughness ABL that deviates significantly from semi-empirical Engineering Sciences Data Unit (ESDU) 85020 model derived for open country and urban terrains with larger surface roughness heights. Although the model accurately predicts the integral length scales non-dimensionalised relative to the boundary layer thickness for the majority of the profile, they are over-predicted by more than double in the lowest 10% of the ABL, corresponding to the atmospheric surface layer (ASL). The analysis shows that the largest eddies at lower heights in the ASL over a very low roughness desert terrain have length scales similar to the characteristic lengths of physical structures positioned on the ground, which corresponds to the maximum wind loads for buildings. Hence, it is recommended that the integral length scales in the ASL are characterised over an estimated range at each of the four terrain categories in AS/NZS 1170.2 to ensure that buildings and other large physical structures can be optimised in terms of their size and location.

Introduction

Wind codes and standards for low- to medium-rise buildings adopt a simplified gust factor approach that assumes quasi-steady wind loads based on a maximum gust wind speed, which can lead to significant errors for very tall buildings with large dynamic responses to the large amplitude fluctuations during high-wind events such as gusts over short time intervals (Mendis et al., 2007). Current design methods in AS/NZS 1170.2 for estimating the peak wind loads on buildings are based on the peak wind speed associated with gusts over a short duration known as the gust period. Analysis of quasi-static wind loads by Emes et al. (2015) found that the the cost of heliostats in a concentrating solar thermal (CST) power tower plant becomes significant at design wind speeds above 10 m/s, beyond which a 5 m/s increase in design wind speed leads to a 34% increase in the total capital cost of a 120 m² heliostat. The frequency of gusts in the ABL has been accounted for by the gust factor method, however the length scales of turbulent eddies relative to the characteristic length of the structure is also known to significantly affect the peak wind loads (Holdø et al., 1982). Small eddies result in pressures on various parts of a structure that become uncorrelated with distance of separation, however large eddies whose size is comparable with the structure result in well correlated pressures over its surface, leading to maximum wind loads (Greenway, 1979; Mendis et al., 2007). Galloping and torsional flutter tend to occur when the turbulent eddies are comparable to the size of the body at small frequencies of the order of 1 Hz (Nakamura, 1993), which corresponds to the natural frequency of large buildings in the ABL (Arakawa and Yamamoto, 2004). Hence, consideration of the size of large-scale eddies in the ABL relative to the characteristic length of the structure can lead to significant savings in costs due to the reduced design wind loading.

The size of the largest eddies in the ABL has a significant effect on the fluctuating pressures on structures, which can result in fatigue damage and can lead to structural collapse. The integral length scale is a measure of the longest correlation distance between two points in the flow field that are separated by either distance or time (O'Neill et al., 2004). The longitudinal integral length scale xL_u is defined in Figure 1 at a given height z in the ABL as the streamwise spacing between two-dimensional spanwise eddies orientated in the axial direction (Emes et al., 2016). Holdø et al. (1982) found that the maximum base pressure coefficient on wind tunnel models of low-rise buildings of height D occurs at $^xL_u/D \approx 2.8$ when exposed to turbulence in the ABL compared to $^xL_u/D \approx 1.6$ for a uniform approaching flow. Designing for the larger ratio results in a 10% increase in drag coefficient on low-rise buildings (Holdø et al., 1982). Hence, the overall aim of this paper is to calculate longitudinal integral length scales using the autocorrelation function in a low-roughness ABL to determine the accuracy of a semi-empirical Engineering Sciences Data Unit (2002) model. This will be used to provide recommendations for improving the accuracy and versatility of the current methods in AS/NZS 1170.2 for calculating wind loads on permanent structures exposed to gusty wind conditions in the ABL.

Atmospheric Boundary Layer Characteristics

Records of wind velocities show that there are gusts or highly turbulent flow at all heights in the ABL, including the lowest 10% of the ABL known as the atmospheric surface layer (ASL) where permanent building structures are positioned on the ground. Turbulent phenomena such as gusts are very complex, however some characteristics of the fully-developed boundary layer wind over flat homogenous terrain can be modelled mathematically as a stationary random process with a zero mean value (Xu, 2013). The instantaneous wind speed can be decomposed as

$$U(z, t) = \bar{U}(z) + u'(z, t), \tag{1}$$

where $\bar{U}(z)$ is the mean wind speed component at height z above the ground and $u'(z, t)$ is the turbulent wind fluctuation component averaged over the gust period t .

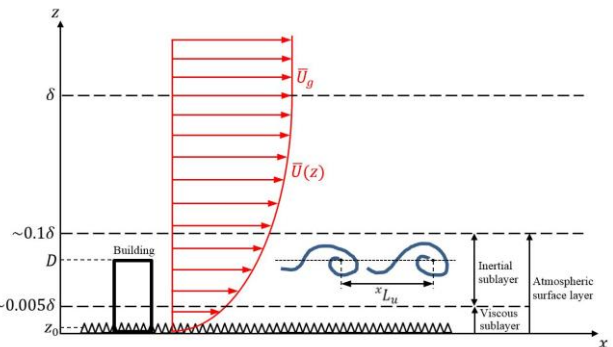


Figure 1. Turbulence characteristics and definition of integral length scale xL_u in the atmospheric boundary layer (Emes et al., 2016).

The mean wind speed profile in the ABL has been modelled to various degrees of accuracy by the power law, logarithmic law and Deaves-Harris model (Mendis et al., 2007). The power law has been found to be appropriate for heights around 30-300m, hence it is commonly used for the calculation of wind loads on buildings and other large structures (Cook, 1997). For the design of structures with height D less than 100m in the ABL, the logarithmic law is most appropriate for modelling the mean velocity profile under the assumption of asymptotic similarity in a neutral ABL (Sun et al., 2014).

$$\bar{U}(z) = \left(\frac{U_\tau}{k}\right) \ln\left(\frac{z}{z_0}\right) \quad (2)$$

Here U_τ (m/s) is the friction velocity representing the Reynolds shear stress $-\rho\overline{u'w'}$ at the surface, k is von Karman's constant (0.4) and z_0 (m) is the surface roughness height as a function of the average height of roughness elements on the ground in Figure 1, which can vary in scale from millimetres in a flat desert to metres in a dense urban area (Xu, 2013). The design wind speed at the height of structures is normally calculated in wind load design codes and standards, such as AS/NZS 1170.2 (Standards Australia, 2011) using an ultimate limit state wind speed with a 5% probability of being exceeded in a 50 year period (Emes et al., 2015; Mendis et al., 2007).

Turbulence intensity is commonly used to describe the level of turbulence in the time domain of the ABL, defined by the ratio of the root-mean-square of the fluctuating component of the instantaneous wind speed and the mean wind speed in Equation (2). However, the distribution of energy in the turbulent flow fluctuations is proposed by similarity theory to give rise to a cascade of eddies spanning a frequency domain and a large range of length scales (Tennekes and Lumley, 1972). Turbulent flow fluctuations are often characterised as coherent eddies in order to simplify the descriptions of the random three-dimensional eddying fluid motions in the ABL over a wide range of length scales. Coherent eddies exist for sufficient time periods to have a significant influence on the time-averaged statistics of a turbulent flow field (Venditti et al., 2013). The size of the largest eddies is defined by the integral length scale xL_u at the lower bound of the inertial subrange frequency domain in the ABL (Kaimal and Finnigan, 1994).

The largest eddies in the ABL are spatially extensive structures that require analysis of many points in space. Point velocity measurements as a function of time are transformed to spatially distributed data by adopting Taylor's hypothesis that eddies are embedded in a frozen turbulence field, which is convected downstream at the mean wind speed \bar{U} (m/s) in the streamwise x direction and hence do not evolve with time (Kaimal and Finnigan, 1994). The integral length scale at a given height in the ABL is therefore calculated as (O'Neill et al., 2004; Swamy et al., 1979).

$$^xL_u = ^xT_u \bar{U}, \quad (3)$$

where xT_u (s) is the integral time scale representing the time taken for the largest eddies to traverse the inertial subrange in the ABL before they are dissipated by viscosity at the Kolmogorov length scale η . Larger integral length scales cause slower variations in the time series and are thus associated with longer integral time scales. Integral time scales are commonly estimated from the covariance of single point velocity data between two different times using the normalised autocorrelation function $R_u(\tau)$ of the fluctuating component of the turbulence velocity (Kaimal and Finnigan, 1994)

$$R_u(\tau) = \frac{\overline{u'(t)u'(t+\tau)}}{\overline{u'(t)u'(t)}} \quad (4)$$

Here τ (s) is the time lag with respect to time t over which $R(\tau)$ decreases in magnitude from one to zero as $u'(t + \tau)$ becomes

uncorrelated and statistically independent of $u'(t)$. The autocorrelation function is calculated from the velocity data using the *xcorr* function in Matlab. The integral time scale is defined by

$$^xT_u = \int_0^\infty R_u(\tau) d\tau \approx \int_0^{\tau_0} R_u(\tau) d\tau, \quad (5)$$

where the integral is taken to the first-zero crossing τ_0 of the autocorrelation function by assuming that $R(\tau)$ fluctuates very close to zero after this point (Swamy et al., 1979). Alternatively xT_u has been approximated by integrating to the point when $R(\tau)$ reaches a value of $1/e \approx 0.37$ or from the frequency at the peak of the Engineering Sciences Data Unit (2002) power spectral density (PSD) function derived from the von Karman spectral equations and fitted to the measured data (Flay and Stevenson, 1988). Analysis of these three methods for calculating xT_u by Flay and Stevenson (1988) showed that xL_u is largely underpredicted in an open country terrain ($z_0 = 30\text{mm}$) because of uncertainties in a fitted model PSD curve. A large portion of the autocorrelation function is not accounted for in the integral to the upper limit $1/e$ (O'Neill et al., 2004). Hence, the first-zero crossing serves as an upper estimate for xL_u that is most appropriate for a low-roughness ABL where smaller xL_u means that $R(\tau)$ will approach zero more quickly (Emes et al., 2016).

Integral Length Scales in a Low-Roughness ABL

High fidelity measurements of wind velocity were acquired from a field experiment study carried out by Hutchins et al. (2012) at the SLTEST facility in the western Utah Great Salt Lake desert. The mean velocity and turbulence intensity profiles lie within a 10% experimental error of the logarithmic law profile in Equation (2) for a mildly transitional rough surface with friction velocity $U_\tau = 0.19$ m/s and equivalent sand grain roughness height $k_s^+ \approx 22$ or surface roughness height $z_0 \approx 1.8\text{mm}$ (Marusic et al., 2013). Velocity data during the field experiment (Hutchins et al., 2012) were obtained during a one hour period of neutral buoyancy and steady wind conditions, such that the velocity profiles are expected to be generated by a shear-driven wall-bounded flow (Marusic and Hutchins, 2008). Velocities were measured using sonic anemometers at logarithmically-spaced heights in the ABL with thickness $\delta \approx 60\text{m}$ estimated from two-point correlations of velocity data and prior radiosonde measurements (Metzger et al., 2007). Sonic anemometers tend to degrade significantly in accuracy at lower heights where the vertical velocity gradients are typically the largest and the eddy scales of interest are too small to be resolved accurately (Kaimal and Finnigan, 1994). However, they are preferred for spectral analysis of integral length scales in the ABL compared to the widely-used cup anemometer. Hence, sonic anemometers are the most appropriate measurement device for dynamic and vibrational responses on buildings and large structures in the ABL arising from the interaction with large eddies of a similar size.

Figure 2 compares the autocorrelation function R_u calculated using Equation (4) at three heights in the low-roughness ABL. The amplitude of the fluctuation of R_u about zero increases with increasing height in the ABL. This indicates that there is a wider range distribution of eddy sizes at larger heights in the ABL. For the analysis of dynamic wind loads on large physical structures, the largest eddies at each height need to be determined. The integral time scales are calculated using Equation (5) for the following three domains:

1. Integrate over the entire domain τ_∞
2. Integrate to the first-zero crossing τ_0
3. Integrate to where R_u falls to $1/e$

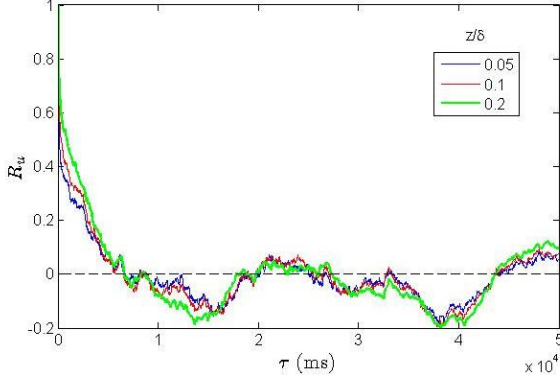


Figure 2. Autocorrelation function $R_u(\tau)$ of velocity data at 3 heights in a low-roughness ABL in Utah, USA.

Figure 3 presents the integral length scales calculated for three different integration domains using velocity data collected by Hutchins et al. (2012) in a low-roughness ABL in Utah, USA. The integration of the full time domain is less than to the first-zero crossing as expected from observation of the significant portion below the x -axis in the autocorrelation functions in Figure 2. Integral length scales are significantly under-predicted, particularly at lower heights, using the third integration domain to $1/e$. This suggests that an insufficient amount of the time domain is covered to capture the size of the largest eddies with low frequencies covered using this method. Comparison of the other two methods shows a 27% difference at the lowest measurement height of 1.42m ($z/\delta = 0.024$) and a 67% difference at the largest measurement height of 25.69m ($z/\delta = 0.43$). These differences in the estimated xL_u show the effect of the fluctuation of R_u after the first-zero crossing. The integral length scale profile calculated to τ_0 follows closer to a linear trend at lower heights, however the profile appears to become more logarithmic when integrating R_u over the whole time domain. The autocorrelation function is expected to decay to zero within a sufficiently large spatial domain, hence the use of the whole domain may lead to erroneous results for xL_u in cases such as Figure 2 where there are random fluctuations in R_u after the first-zero crossing. O'Neill et al. (2004) showed that xL_u becomes independent of the domain size when the spatial domain is at least six times larger than xL_u . In the case of a low-roughness ABL with a sufficiently large spatial domain, the first-zero crossing is the most appropriate integration domain for xT_u where smaller xL_u means that $R(\tau)$ will approach zero more quickly.

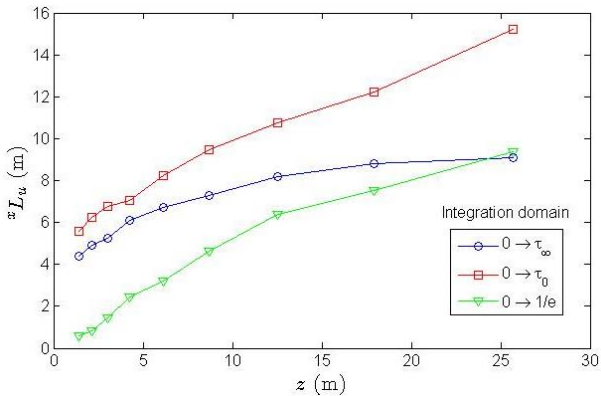


Figure 3. Integral length scales determined using three different integration domains of $R_u(\tau)$ as a function of height z in a low-roughness ABL in Utah, USA.

The majority of integral length scale data available in the literature has been obtained from field-site anemometer velocity measurements in large-scale ABLs, however there are few recognised standards due to the diverse nature and scales of ABLs. Table 1 presents the reference atmospheric conditions for the semi-empirical data developed by Engineering Sciences Data Unit (ESDU) 85020 for the integral length scales of atmospheric turbulence over uniform terrain in a neutral ABL. This data set extends previous empirical formulations for xL_u to higher equivalent design wind speeds up to 30 m/s at heights corresponding to taller buildings for which dynamic effects are more significant (Engineering Sciences Data Unit, 2002). A correction factor k_L is used to account for the variation of xL_u with a change in mean wind speed $\bar{U}_{10r} = 6.19$ m/s at a 10m height in the field experiment ABL (Hutchins et al., 2012) within an estimated $\pm 8\%$ error (Engineering Sciences Data Unit, 2002) such that the integral length scales predicted by the ESDU model can be compared with the field experiment data in Figure 4.

| \bar{U}_{10r} | f | z_0 |
|-----------------|--------------------------|--------|
| 20 m/s | 1×10^{-5} rad/s | 0.03 m |

Table 1. Reference ABL characteristics for ESDU 85020 integral length scale data (Engineering Sciences Data Unit, 2002).

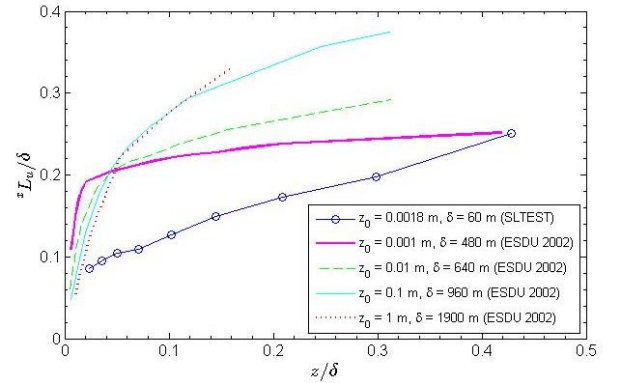


Figure 4. Comparison of integral length scales calculated for a low-roughness ABL with those predicted from ESDU 85020 (2002) correlations as a function of non-dimensional height z/δ in the ABL.

The results from a low-roughness ABL in the field experiment in Figure 4 show that $^xL_u/\delta \approx 0.1$ at $z/\delta \approx 0.05$, corresponding to half that of the predicted $^xL_u/\delta \approx 0.2$ by the ESDU 85020 model (Emes et al., 2016). The linear relationship between xL_u and z in Figure 4 suggests that physical structures positioned on the ground in a low-roughness ABL are exposed to eddies that are a similar size ($^xL_u/D \approx 1$), leading to the maximum wind loads due to turbulent buffeting (Greenway, 1979; Mendis et al., 2007). The significance of the relationship between xL_u and z_0 has major implications for the dynamic wind loads on low-rise buildings exposed to gusts in the ABL, which can lead to 10% over-prediction of the drag coefficient for $I_u = 25\%$ at $z/\delta = 0.1$ (Holdø et al., 1982). The characteristics of low-roughness ABLs appear to differ considerably from urban terrains with larger roughness heights. Further understanding of how unsteady wind loads vary with the ratio $^xL_u/D$ would allow for optimisation of the sizes of buildings and structures based on the largest eddies that they are likely to be exposed to at a given height in the ABL. This could be achieved through full-scale measurements of xL_u at each of the characteristic z_0 values corresponding to the main terrain categories in building design standards. For example, estimation of xL_u at each of the four terrain categories in AS/NZS 1170.2 would ensure that buildings and other large physical structures can be optimised in terms of their size and location.

Changes in surface roughness are shown in Figure 4 to have a significant effect on integral length scales that can vary by as much as an order of magnitude from 10m to 100m, hence the specification of integral length scales in wind load codes and design standards such as AS/NZS 1170.2 would allow for optimisation of the size and location of a physical structure such that the maximum wind loads from the exposure to large eddies of a similar size can be minimised. More accurate prediction of the variation of xL_u with height in the lowest 100m of the ABL is required for low-roughness terrains, which tend to deviate from semi-empirical models developed for high roughness terrains such as urban environments. Calculation of the estimated range of integral length scales from sonic anemometer velocity measurements at each of the four terrain categories in AS/NZS 1170.2 ($z_0 = 0.002\text{m}, 0.02\text{m}, 0.2\text{m}, 2\text{m}$) would ensure that buildings and other large structures are not overdesigned following Engineering Sciences Data Unit (2002) models that predict eddies over double the size of those that exist in low-roughness ABLs.

Conclusions

Longitudinal integral length scales in the lowest 10% of the ABL predicted by the Engineering Sciences Data Unit (2002) model are over double those calculated from autocorrelation of velocity measurements in a low-roughness ABL in the Utah desert. Although ESDU correlations have been shown to be an upper bound on integral length scales calculated in full-scale ABLs, the predicted logarithmic relationship with non-dimensional height in the ABL is not appropriate for low-roughness ABLs where a linear relationship is observed. The sizes of the largest eddies that physical structures are exposed to at a given height in the ABL are not taken into account in the calculation of design wind loads in wind codes and standards following the quasi-steady gust factor method. However, knowledge of the estimated size of the largest eddies that a physical structure is exposed to at a given location can assist in the optimisation of the critical scaling parameters of the structure during the design stage. The present analysis shows that the largest eddies at lower heights in the ASL over a very low roughness desert terrain have length scales similar to the characteristic lengths of physical structures positioned on the ground, which corresponds to the maximum wind loads for buildings.

Acknowledgments

The authors would like to acknowledge Nicholas Hutchins and others at the University of Melbourne for their contribution of velocity data obtained from the SLTEST facility in Utah, USA. Support for the work has been provided by the Australian Solar Thermal Research Initiative (ASTRI), through funding provided by the Australian Renewable Energy Agency (ARENA).

References

Arakawa, T., Yamamoto, K., 2004, Frequencies and damping ratios of a high rise building based on microtremor measurement, in: Proc., 13 th World Conference on Earthquake Engineering.

Cook, N.J., 1997, The Deaves and Harris ABL model applied to heterogeneous terrain, *Journal of Wind Engineering and Industrial Aerodynamics* 66, 197-214.

Emes, M.J., Arjomandi, M., Kelso, R.M., Ghanadi, F., 2016, Understanding of the relationship between gust factor, turbulence intensity and integral length scales in the atmospheric boundary layer, submitted to *Journal of Wind Engineering and Industrial Aerodynamics*.

Emes, M.J., Arjomandi, M., Nathan, G.J., 2015, Effect of heliostat design wind speed on the levelised cost of electricity from concentrating solar thermal power tower plants, *Solar Energy* 115, 441-451.

Engineering Sciences Data Unit, 2002, Characteristics of atmospheric turbulence near the ground - Part II: single point data for strong winds (neutral atmosphere), London, ESDU 85020.

Flay, R., Stevenson, D., 1988, Integral length scales in strong winds below 20 m, *Journal of Wind Engineering and Industrial Aerodynamics* 28, 21-30.

Greenway, M., 1979, An analytical approach to wind velocity gust factors, *Journal of Wind Engineering and Industrial Aerodynamics* 5, 61-91.

Holdø, A., Houghton, E., Bhinder, F., 1982, Some effects due to variations in turbulence integral length scales on the pressure distribution on wind-tunnel models of low-rise buildings, *Journal of Wind Engineering and Industrial Aerodynamics* 10, 103-115.

Hutchins, N., Chauhan, K., Marusic, I., Monty, J., Klewicki, J., 2012, Towards reconciling the large-scale structure of turbulent boundary layers in the atmosphere and laboratory, *Boundary-layer meteorology* 145, 273-306.

Kaimal, J.C., Finnigan, J.J., 1994, Atmospheric boundary layer flows: their structure and measurement,

Marusic, I., Hutchins, N., 2008, Study of the log-layer structure in wall turbulence over a very large range of Reynolds number, *Flow, Turbulence and Combustion* 81, 115-130.

Marusic, I., Monty, J.P., Hultmark, M., Smits, A.J., 2013, On the logarithmic region in wall turbulence, *Journal of Fluid Mechanics* 716, R3.

Mendis, P., Ngo, T., Haritos, N., Hira, A., Samali, B., Cheung, J., 2007, Wind loading on tall buildings, *EJSE Special Issue: Loading on Structures* 3, 41-54.

Metzger, M., McKeon, B., Holmes, H., 2007, The near-neutral atmospheric surface layer: turbulence and non-stationarity, *Philosophical Transactions of the Royal Society of London A: Mathematical, Physical and Engineering Sciences* 365, 859-876.

Nakamura, Y., 1993, Bluff-body aerodynamics and turbulence, *Journal of Wind Engineering and Industrial Aerodynamics* 49, 65-78.

O'Neill, P., Nicolaides, D., Honnery, D., Soria, J., 2004, Autocorrelation functions and the determination of integral length with reference to experimental and numerical data, in: 15th Australasian Fluid Mechanics Conference The University of Sydney, Sydney, Australia, pp. 13-17.

Standards Australia, 2011, Structural design actions, Part 2: Wind actions, AS/NZS 1170.2.

Sun, H., Gong, B., Yao, Q., 2014, A review of wind loads on heliostats and trough collectors, *Renewable and Sustainable Energy Reviews* 32, 206-221.

Swamy, N., Gowda, B., Lakshminath, V., 1979, Auto-correlation measurements and integral time scales in three-dimensional turbulent boundary layers, *Applied Scientific Research* 35, 237-249.

Tennekes, H., Lumley, J.L., 1972, A first course in turbulence, MIT press.

Venditti, J.G., Best, J.L., Church, M., Hardy, R.J., 2013, Coherent Flow Structures at Earth's Surface, John Wiley & Sons.

Xu, Y.L., 2013, Wind Characteristics in Atmospheric Boundary Layer, *Wind Effects on Cable-Supported Bridges* 25-59.